Electronic Supplementary Material (ESI) for Green Chemistry.

Supplementary data

A sustainable preparation of catalytically active and antibacterial cellulose metal nanocomposites via ball-milling of cellulose

Joanna Kwiczak-Yiğitbaşı,[a] Özge Laçin,[a] Mine Demir,[a] Recep Erdem Ahan,[b] Urartu Özgür Şafak Şeker,[b] and Bilge Baytekin[*a,b]

[a] Chemistry Department, Bilkent University, 06800, Ankara, TURKEY

[b] UNAM, Bilkent University, 06800, Ankara, TURKEY

* Corresponding author:

E-mail: b-baytekin@fen.bilkent.edu.tr

Supplementary text:

Atomic percentage (at. %) of the metals in the nanocomposites in Table S1 were calculated based on the peak's area evaluated from XPS survey for each nanocomposite. Following sensitivity factors were used for the calculations: 2.881 (O1s), 1.000 (C1s), 20.735 (Au4f), 22.131 (Ag4d), 16.678 (Pt4f), 7.943 (Pd3d). Atomic percentage is an average of at least 4 independent XPS measurements.

Figure S1. Cryomill instrument used for the preparation of cellulose-based nanocomposites.

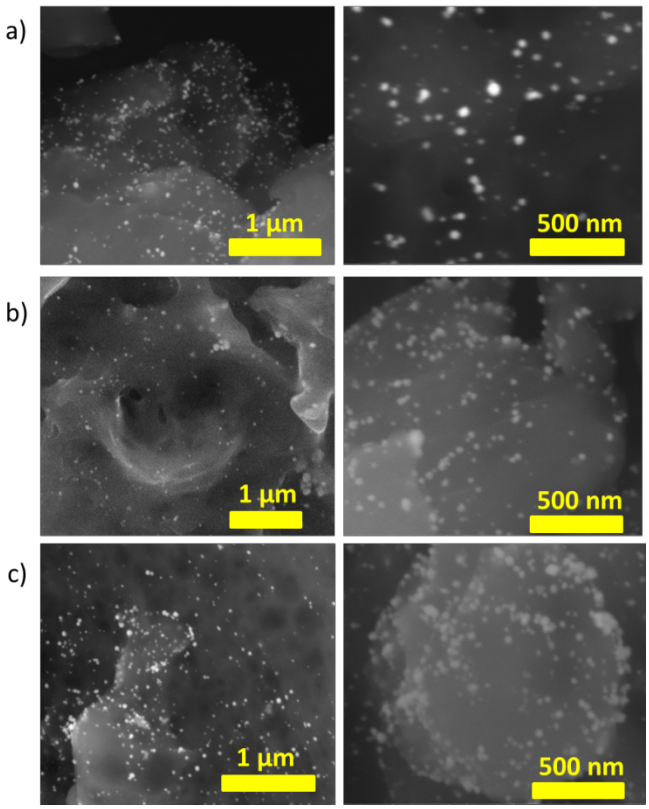

Figure S2. SEM images of cotton-Au NPs prepared by grinding 0.5 g of cotton at 30 Hz frequency in the presence of 6 zirconia balls in the zirconia sample chamber at 77 K for 30 minutes and then, adding $HAuCl_4$ solution in H_2O (3 mL, $5.1x10^{-3}$ M) (See Experimental section for more details). SEM images were taken after a) 1 day, b) 1 week, c) 2 weeks of storing the sample in $HAuCl_4$ solution in H_2O. The images show that neither Au NPs size nor Au NPs concentration (as shown quantitatively by XPS measurements, Table S1) change within the storing time.

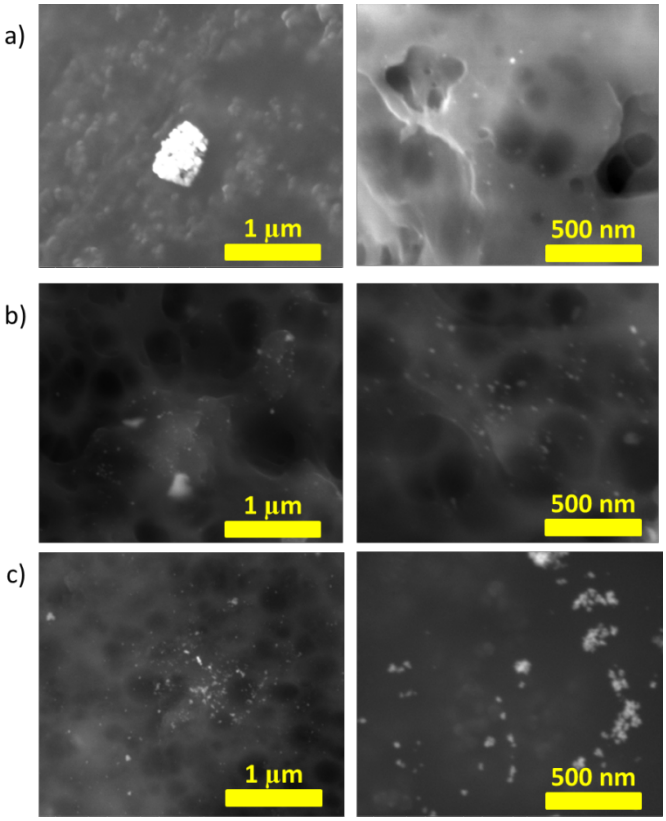

Figure S3. SEM images of cotton-Ag NPs prepared by grinding 0.5 g of cotton at 30 Hz frequency in the presence of 6 zirconia balls in the zirconia sample chamber at 77 K for 30 minutes and then, adding $AgNO_3$ solution in H_2O (3 mL, $5.1x10^{-3}$ M) (See Experimental section for more details). SEM images were taken after a) 1 day, b) 1 week, c) 2 weeks of storing the sample in $AgNO_3$ solution in H_2O. The images show that Ag NPs size does not change within the time however, the concentration of Ag NPs (as shown quantitatively by XPS measurements, Table S1) is increasing within the storage time.

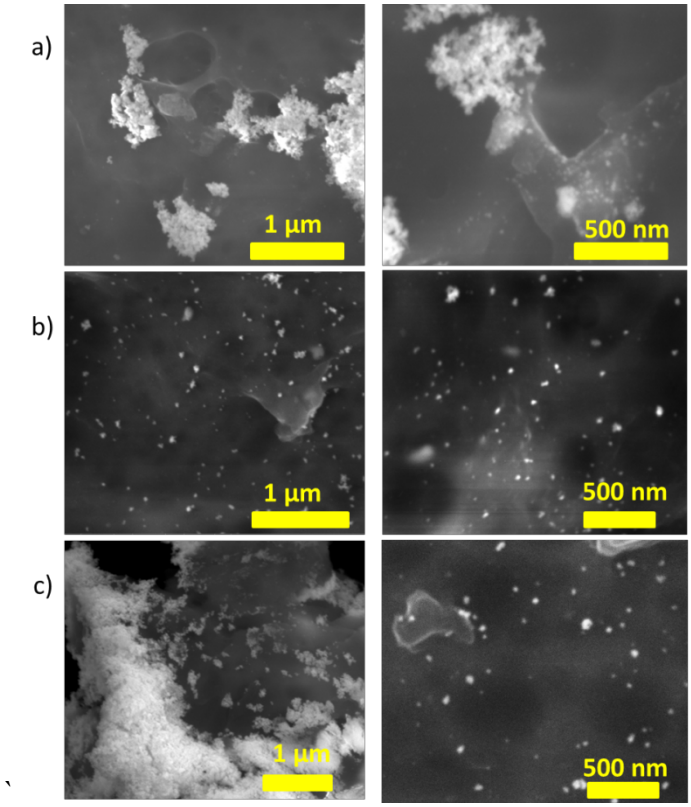

Figure S4. SEM images of cotton-Pt NPs prepared by grinding 0.5 g of cotton at 30 Hz frequency in the presence of 6 zirconia balls in the zirconia sample chamber at 77 K for 30 minutes and then, adding K_2PtCl_4 solution in H_2O (3 mL, $5.1x10^{-3}$ M) (See Experimental section for more details). SEM images were taken after a) 1 day, b) 1 week, c) 2 weeks of storing the sample in K_2PtCl_4 solution in H_2O. The images show that Pt NPs size does not change within the time however, the concentration of Pt NPs (as shown quantitatively by XPS measurements, Table S1) is increasing within the storage time.

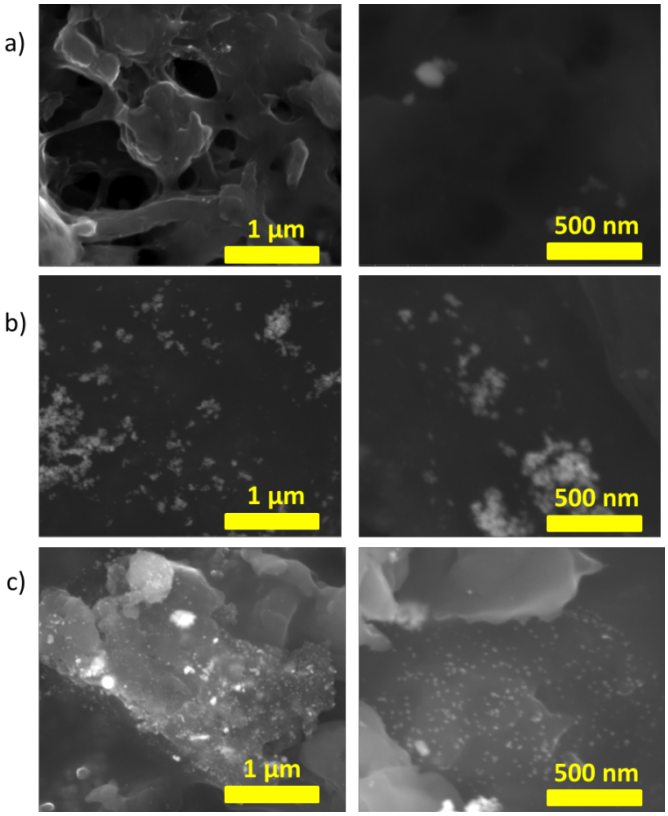

Figure S5. SEM images of cotton-Pd NPs prepared by grinding 0.5 g of cotton at 30 Hz frequency in the presence of 6 zirconia balls in the zirconia sample chamber at 77 K for 30 minutes and then, adding $Pd(C_5H_7O_2)_2$ solution in acetonitrile (3 mL, $5.1x10^{-3}$ M) (See Experimental section for more details). SEM images were taken after a) 1 day, b) 1 week, c) 2 weeks of storing the sample in $Pd(C_5H_7O_2)_2$ solution in acetonitrile. The images show that Pd NPs size does not change within the time however, the concentration of Pd NPs (as shown quantitatively by XPS measurements, Table S1) is increasing within the storage time.

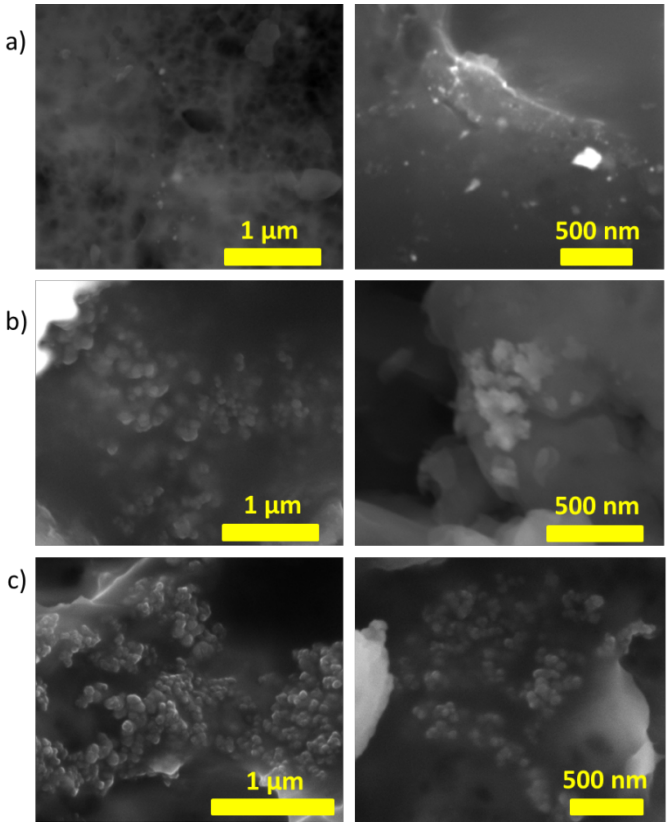

Figure S6. SEM images of cotton-Co NPs prepared by grinding 0.5 g of cotton at 30 Hz frequency in the presence of 6 zirconia balls in the zirconia sample chamber at 77 K for 30 minutes and then, adding $Co(C_5H_7O_2)_2$ solution in acetonitrile (3 mL, $5.1x10^{-3}$ M) (See Experimental section for more details). SEM images were taken after a) 1 day, b) 1 week, c) 2 weeks of storing the sample in $Co(C_5H_7O_2)_2$ solution in acetonitrile. The images show that Co NPs size does not change within the time however, the concentration of Co NPs is increasing within the storage time.

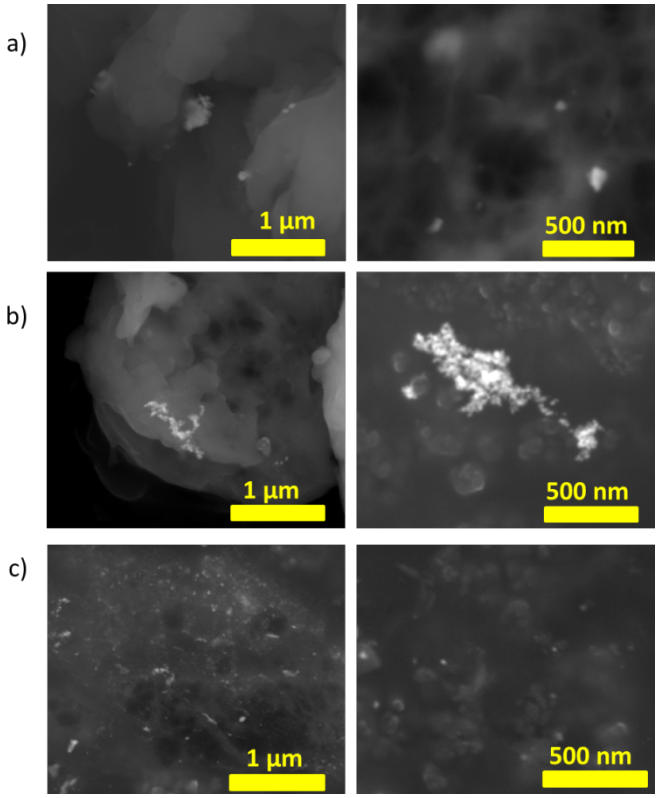

Figure S7. SEM images of cotton-Cu NPs prepared by grinding 0.5 g of cotton at 30 Hz frequency in the presence of 6 zirconia balls in the zirconia sample chamber at 77 K for 30 minutes and then, adding $Cu(C_5H_7O_2)_2$ solution in acetonitrile (3 mL, $5.1x10^{-3}$ M) (See Experimental section for more details). SEM images were taken after a) 1 day, b) 1 week, c) 2 weeks of storing the sample in $Cu(C_5H_7O_2)_2$ solution in acetonitrile. The images show that Cu NPs size does not change within the time however, the concentration of Cu NPs is increasing within the storage time.

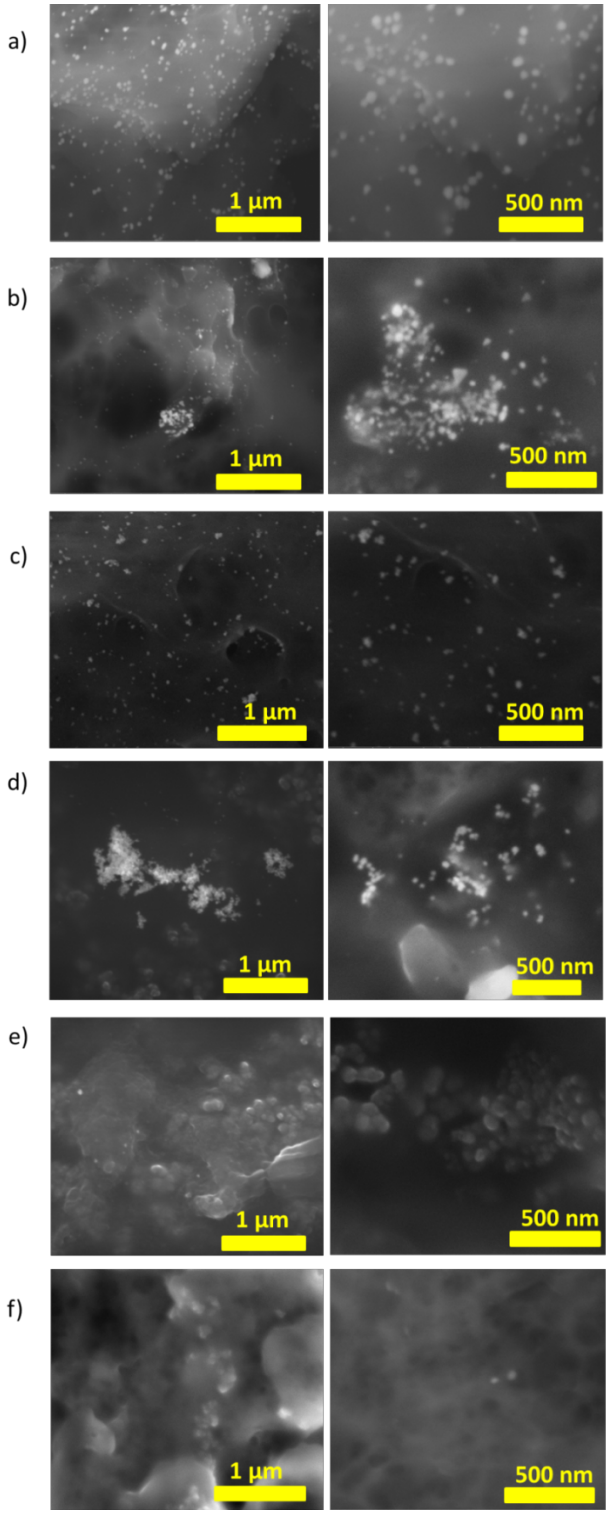

Figure S8. SEM images of a) MCC-Au, b) MCC-Ag, c) MCC-Pt, d) MCC-Pd, e) MCC-Co, and f) MCC-Cu NPs, prepared by grinding 0.5 g of MCC at 30 Hz frequency in the presence of 6 zirconia balls in the zirconia sample chamber at 77 K for 30 minutes and then, adding metal ion solution (3 mL, 5.1×10^{-3} M, $HAuCl_4$, K_2PtCl_4, $AgNO_3$ in H_2O; $Co(C_5H_7O_2)_2$, $Cu(C_5H_7O_2)_2$, $Pd(C_5H_7O_2)_2$ in acetonitrile) (See Experimental section for more details). SEM images were taken after 2 weeks of storing the sample in the corresponding metal ion solution.

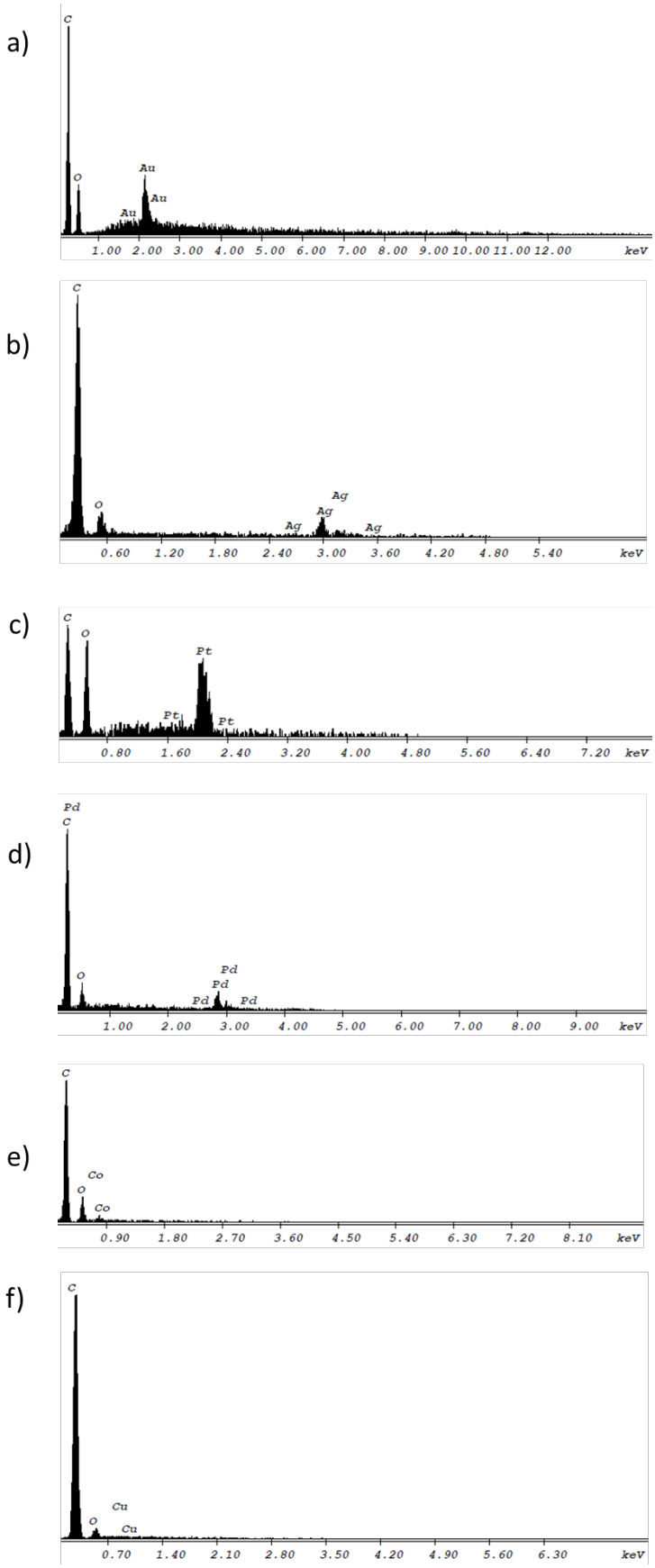

Figure S9. EDX spectra of a) MCC-Au, b) MCC-Ag, c) MCC-Pt, d) MCC-Pd, e) MCC-Co, and f) MCC-Cu nanocomposites.

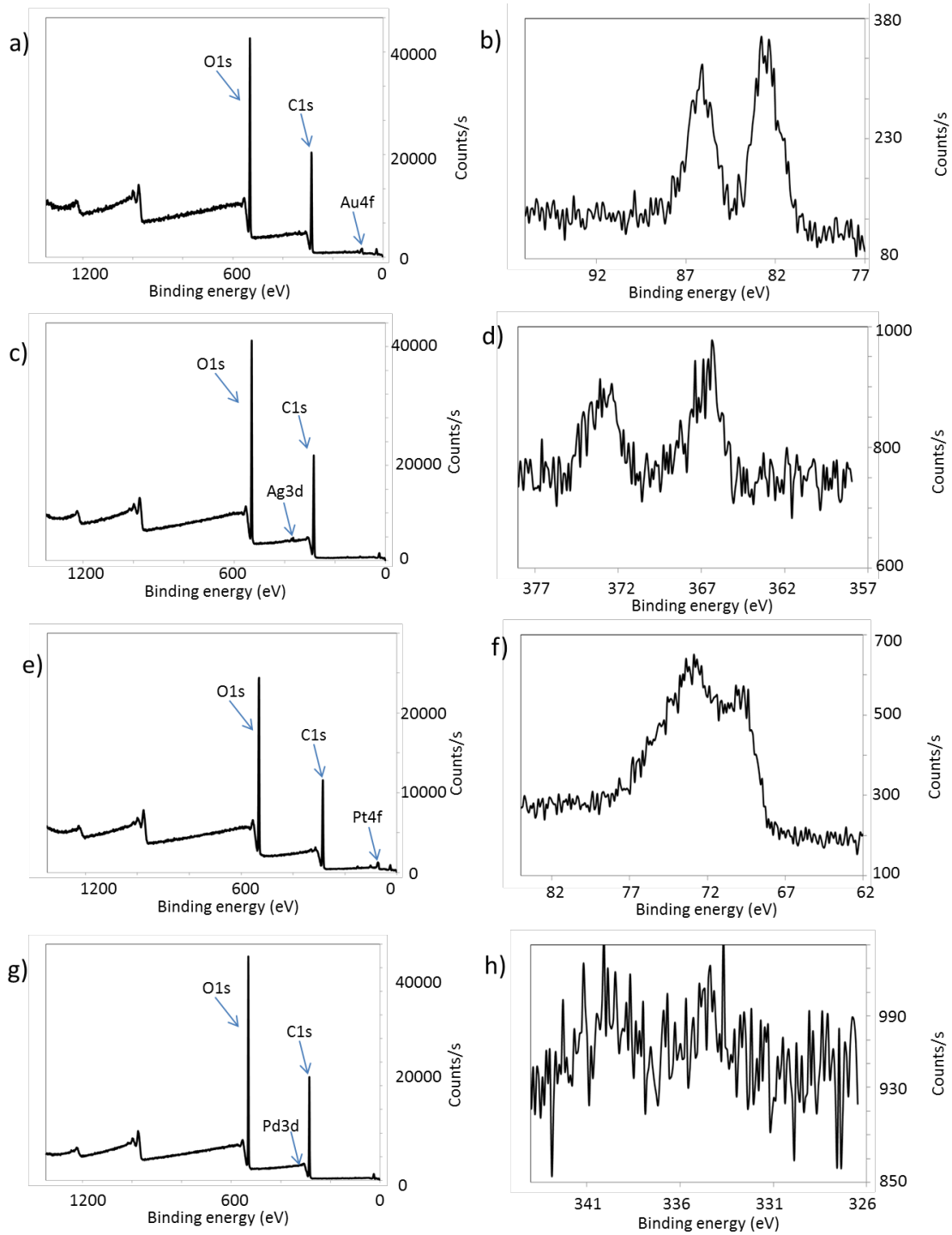

Figure S10. XPS survey of a) cotton-Au, c) cotton-Ag, e) cotton-Pt, g) cotton-Pd, and HIRES XPS spectra of b) cotton-Au, d) cotton-Ag, f) cotton-Pt, h) cotton-Pd nanocomposites prepared by grinding 0.5 g of cotton at 30 Hz frequency in the presence of 6 zirconia balls in the zirconia sample chamber at 77 K for 30 minutes and then, adding metal ion solution (3 mL, 5.1×10^{-3} M, $HAuCl_4$, K_2PtCl_4, $AgNO_3$ in H_2O; $Pd(C_5H_7O_2)_2$ in acetonitrile) (See Experimental section for more details). These spectra verify the metallic nature of the nanoparticles – the successful reduction of the metal ion by the mechanoradicals.

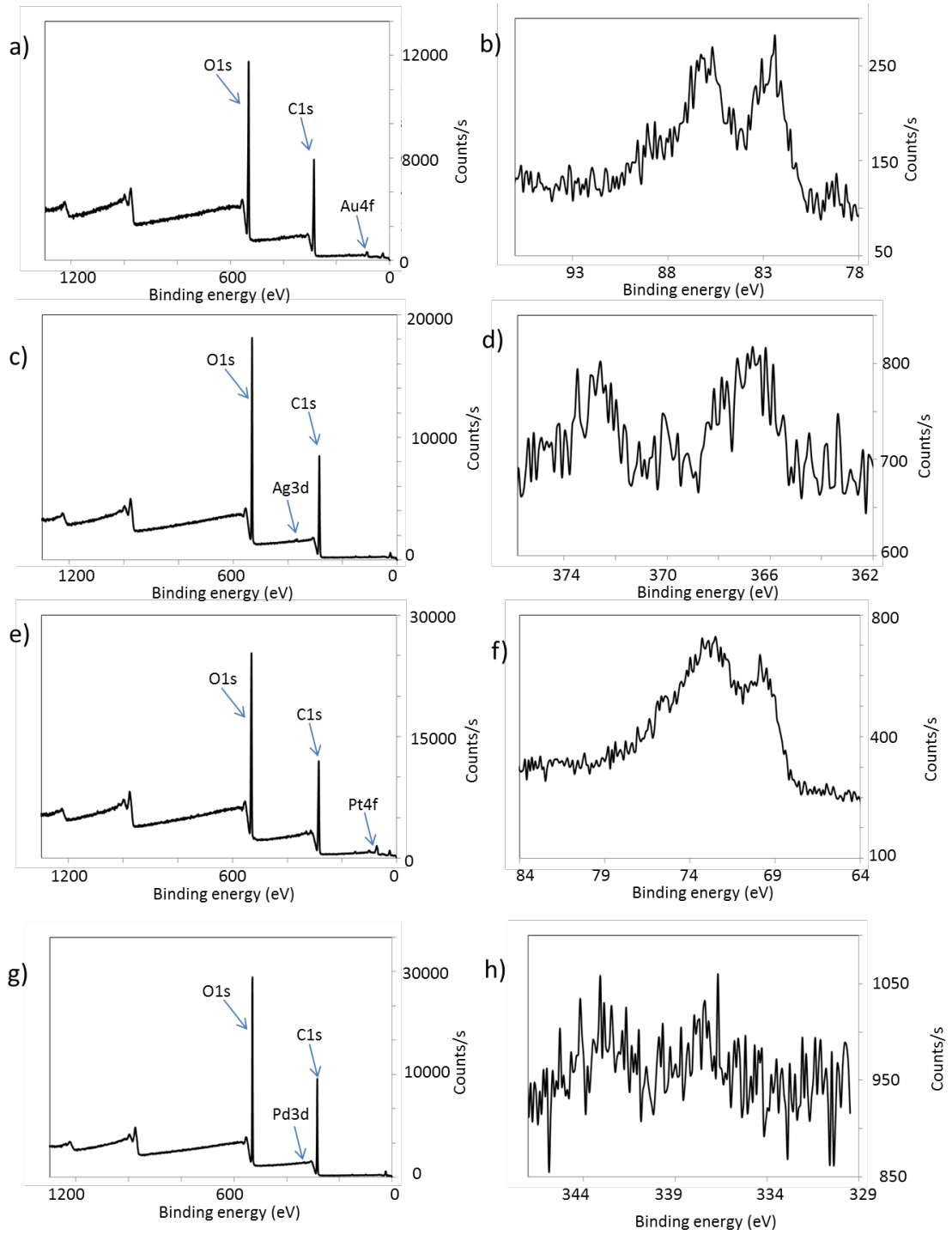

Figure S11. XPS survey of a) MCC-Au, c) MCC-Ag, e) MCC-Pt, g) MCC-Pd, and HIRES XPS spectra of b) MCC-Au, d) MCC-Ag, f) MCC-Pt, h) MCC-Pd nanocomposites prepared by grinding 0.5 g of MCC at 30 Hz frequency in the presence of 6 zirconia balls in the zirconia sample chamber at 77 K for 30 minutes and then, adding metal ion solution (3 mL, 5.1×10^{-3} M, $HAuCl_4$, K_2PtCl_4, $AgNO_3$ in H_2O; $Pd(C_5H_7O_2)_2$ in acetonitrile) (See Experimental section for more details). These spectra verify the metallic nature of the nanoparticles – the successful reduction of the metal ion by the mechanoradicals.

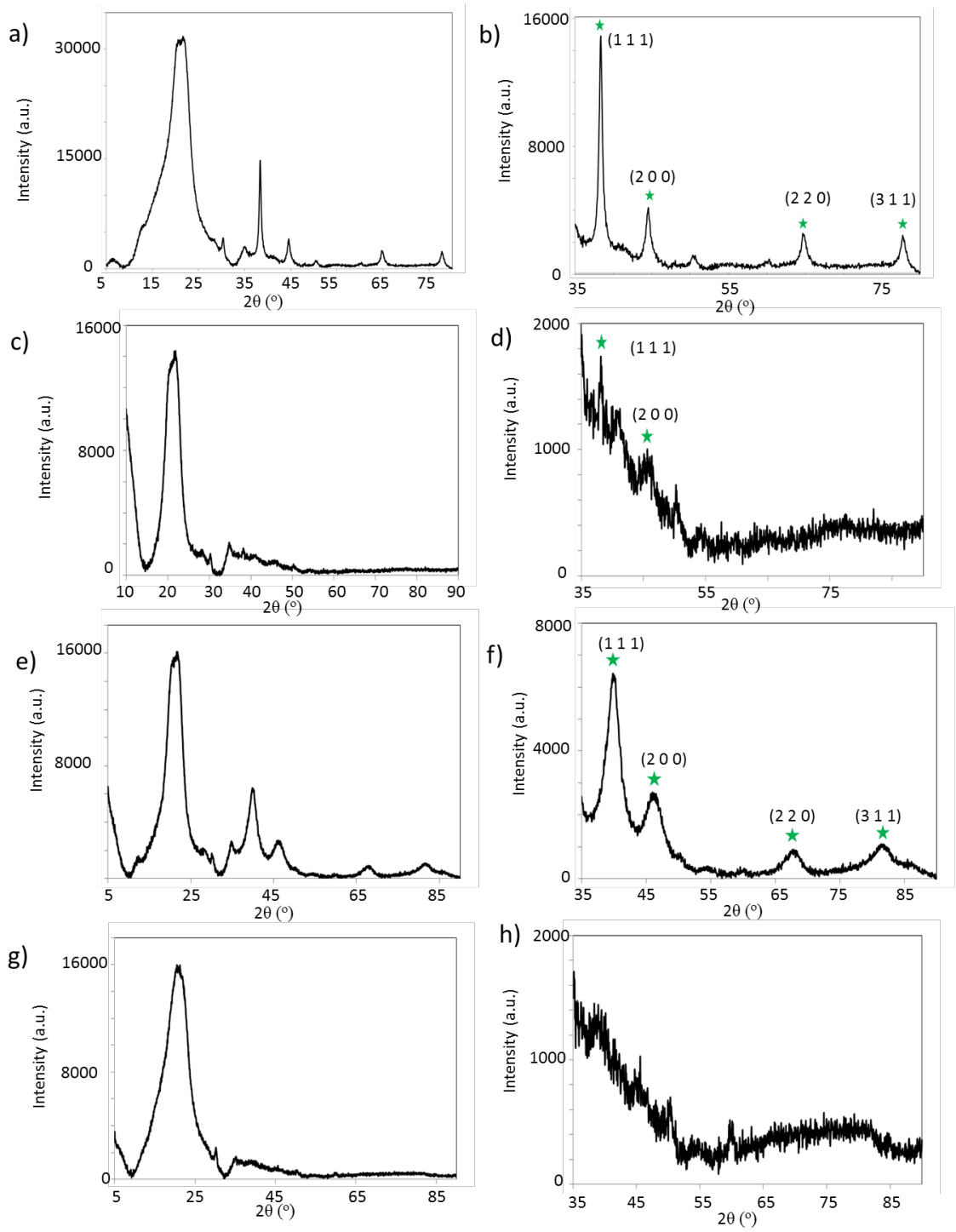

Figure S12. X-Ray diffractograms of a) and b) cotton-Au, c) and d) cotton-Ag, e) and f) cotton-Pt, g) and h) cotton-Pd nanocomposites prepared by grinding 0.5 g of cotton at 30 Hz frequency in the presence of 6 zirconia balls in the zirconia sample chamber at 77 K for 30 minutes and then, adding metal ion solution (3 mL, 5.1×10^{-3} M, $HAuCl_4$, K_2PtCl_4, $AgNO_3$ in H_2O; $Pd(C_5H_7O_2)_2$ in acetonitrile) (See Experimental section for more details). These diffractograms verify the metallic nature of the nanoparticles – the successful reduction of the metal ion by the mechanoradicals, as evidenced by the appearance of the signals at the star labelled diffraction angles.

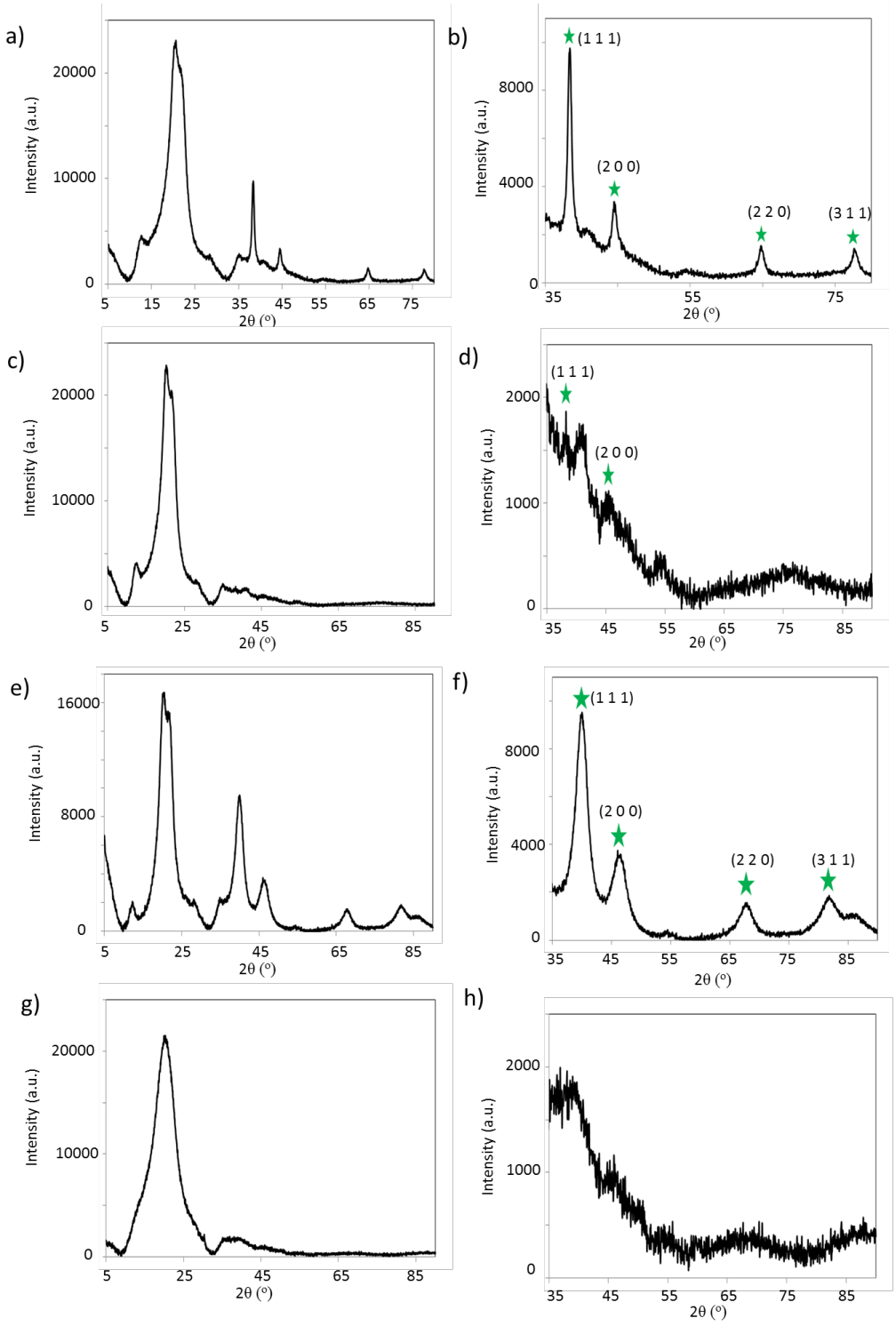

Figure S13. X-Ray diffractograms of a) and b) MCC-Au, c) and d) MCC-Ag, e) and f) MCC-Pt, g) and h) MCC-Pd nanocomposites prepared by grinding 0.5 g of MCC at 30 Hz frequency in the presence of 6 zirconia balls in the zirconia sample chamber at 77 K for 30 minutes and then, adding metal ion solution (3 mL, 5.1×10^{-3} M, $HAuCl_4$, K_2PtCl_4, $AgNO_3$ in H_2O; $Pd(C_5H_7O_2)_2$ in acetonitrile) (See Experimental section for more details). These diffractograms verify the metallic nature of the nanoparticles – the successful reduction of the metal ion by the mechanoradicals, as evidenced by the appearance of the signals at the star labelled diffraction angles.

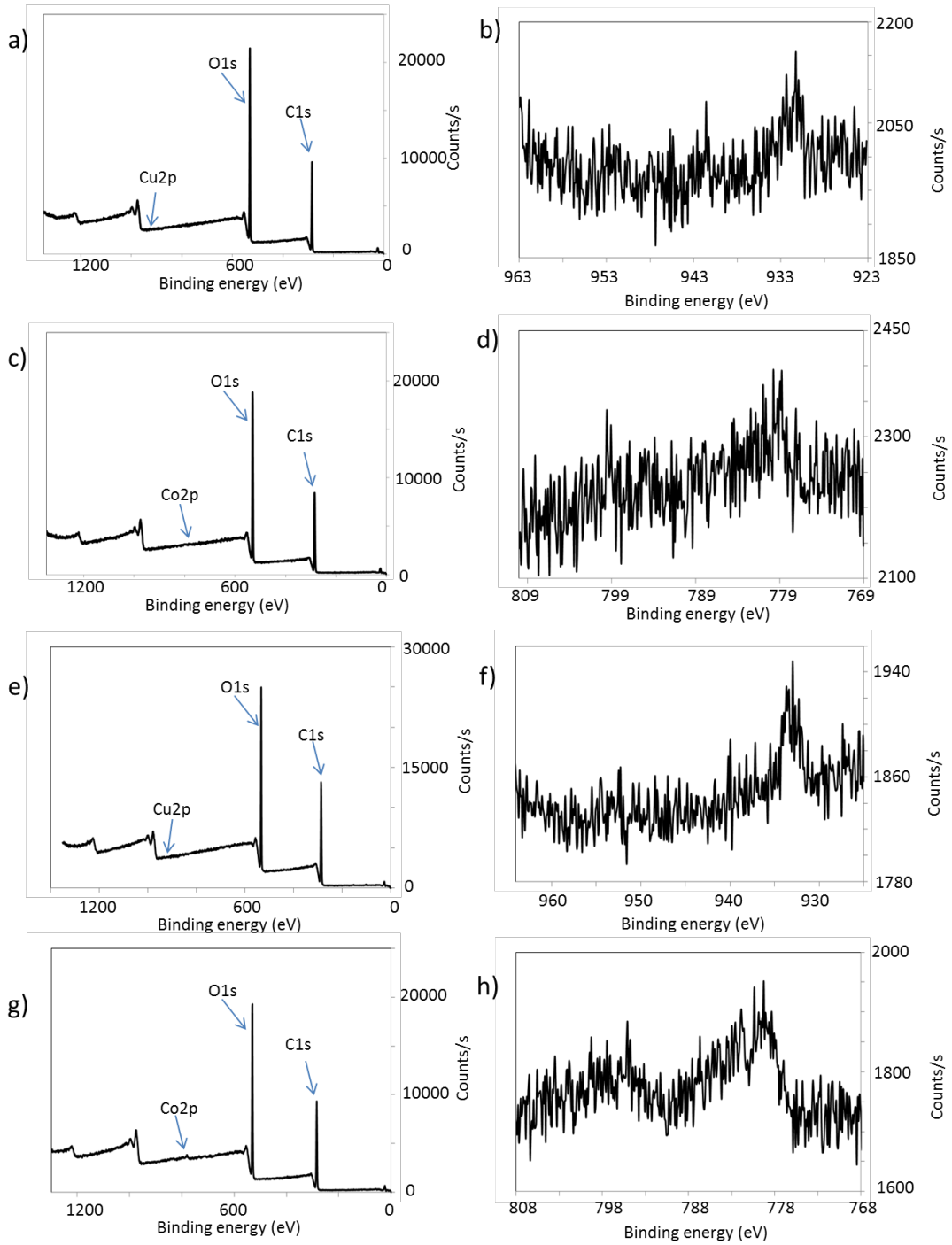

Figure S14. XPS survey of a) cotton-Cu, c) cotton-Co, e) MCC-Cu, g) MCC-Co, and HIRES XPS spectra of b) cotton-Cu, d) cotton-Co, f) MCC-Cu, h) MCC-Co nanocomposites prepared by grinding 0.5 g of cotton/MCC at 30 Hz frequency in the presence of 6 zirconia balls in the zirconia sample chamber at 77 K for 30 minutes and then, adding metal ion solution (3 mL, 5.1×10^{-3} M, $Co(C_5H_7O_2)_2$, $Cu(C_5H_7O_2)_2$ in acetonitrile) (See Experimental section for more details).

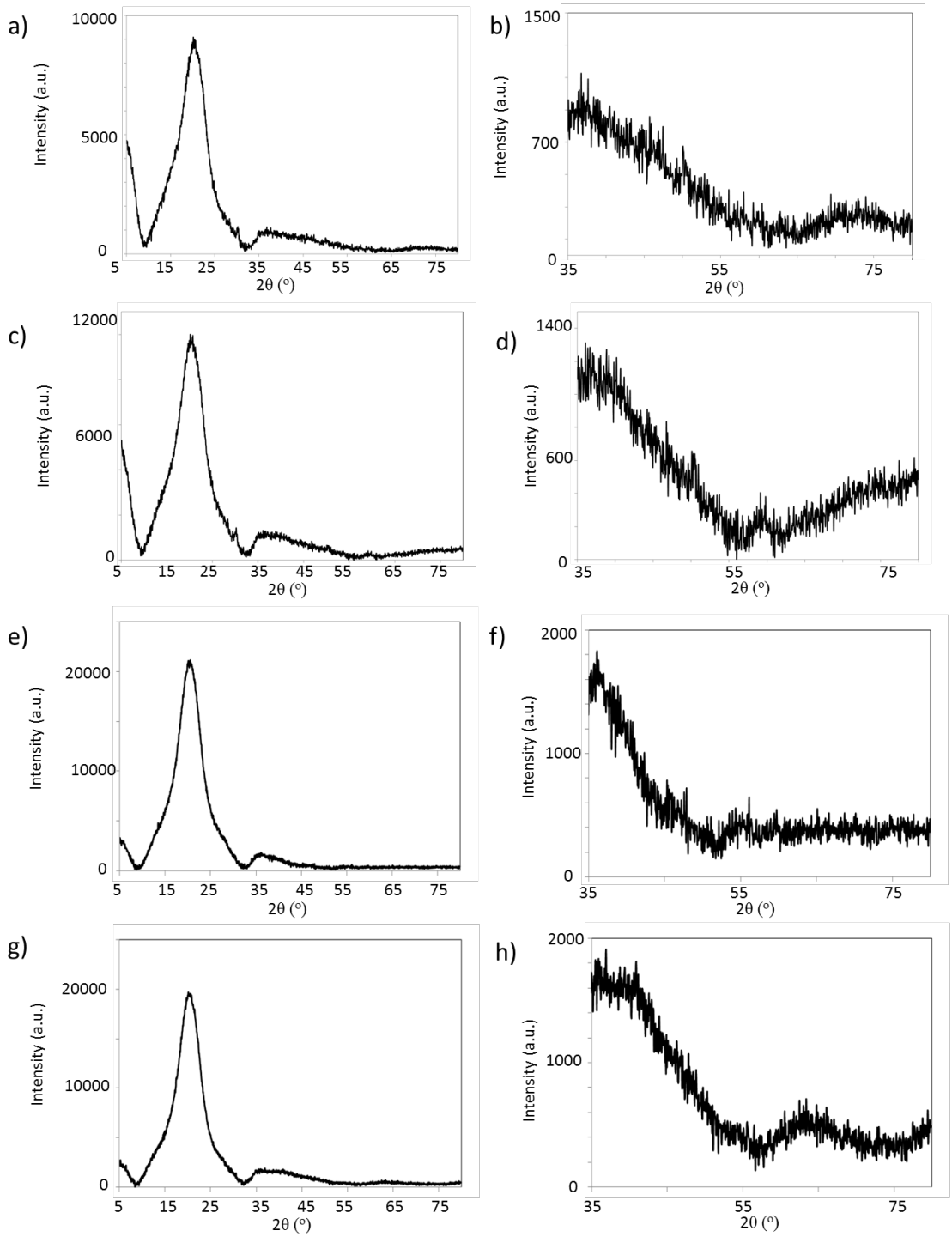

Figure S15. X-Ray diffractograms of a) and b) cotton-Cu, c) and d) cotton-Co, e) and f) MCC-Cu, g) and h) MCC-Co nanocomposites prepared by grinding 0.5 g of cotton/MCC at 30 Hz frequency in the presence of 6 zirconia balls in the zirconia sample chamber at 77 K for 30 minutes and then, adding metal ion solution (3 mL, 5.1×10^{-3} M, $Co(C_5H_7O_2)_2$, $Cu(C_5H_7O_2)_2$ in acetonitrile) (See Experimental section for more details).

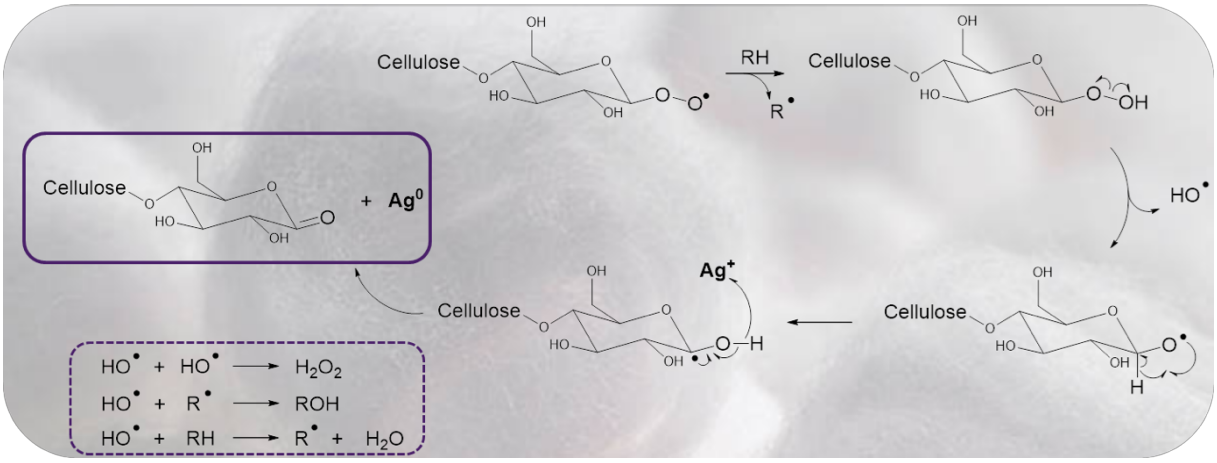

Figure S16. Proposed mechanism of the reduction of metal ions to the metal nanoparticles. In the first step, cellulose peroxy radicals can abstract H$^{\bullet}$ from CH/CH$_2$ groups present in cellulose to form peroxides, –COOH. Peroxides are known to be unstable, thus they decompose to alkoxy (CO$^{\bullet}$), and hydroxyl (HO$^{\bullet}$) radicals.[1] Alkoxy radicals may transform to carbon-centered radicals, which can reduce metal ions to their metallic form.[2–4] This mechanism is additionally supported by FTIR-ATR spectra of the ground cellulose and the final nanocomposites showing a new signal at 1650 cm^{-1} appears after milling (Figure S17, S18).

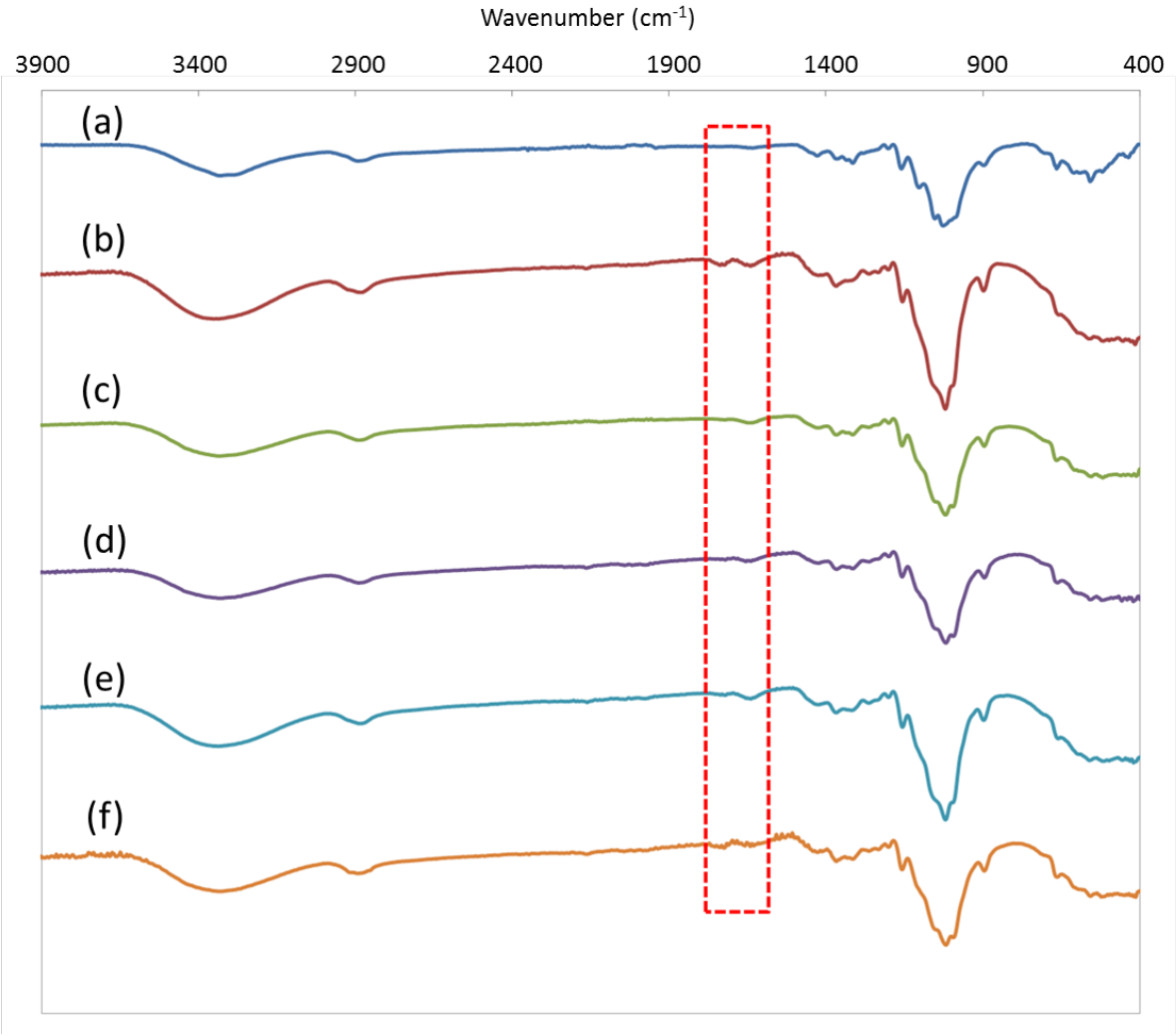

Figure S17. FTIR-ATR spectra of a) native cotton, b) cryomilled cotton (for 30 minutes, at 30 Hz), and c) cotton-Ag, d) cotton-Pt, e) cotton-Pd, f) cotton-Au nanocomposites. Spectra show that during grinding and after addition of metal ion precursors new signals at 1650 cm^{-1} (C=O stretching) appear, which confirm that cellulose is being oxidized during milling.

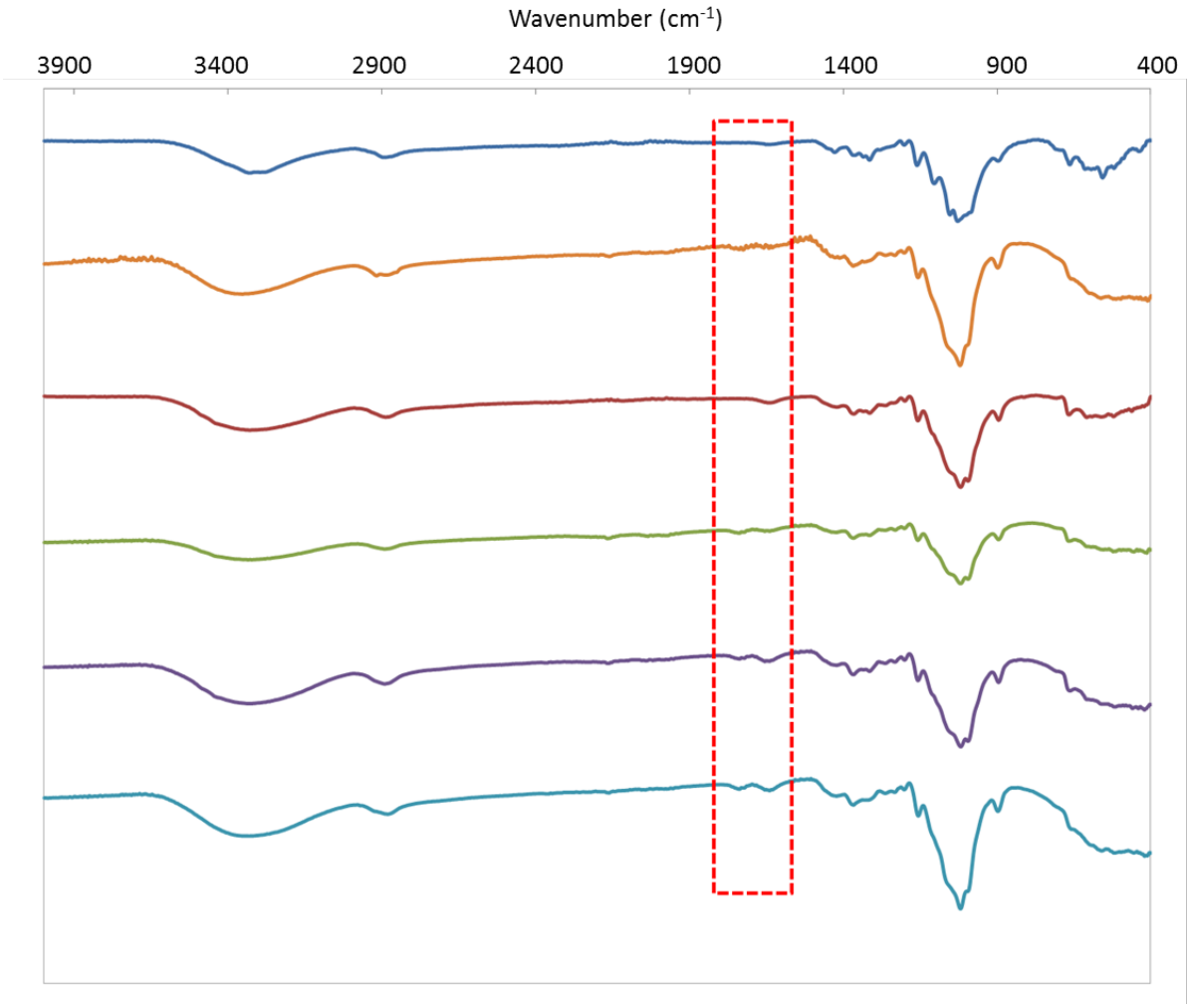

Figure S18. FTIR-ATR spectra of a) MCC, b) cryomilled MCC (for 30 minutes, at 30 Hz), and c) MCC-Au, d) MCC-Ag, e) MCC-Pt, f) MCC-Pd nanocomposites. Spectra show that during grinding and after addition of metal ion precursors new signals at 1650 cm^{-1} (C=O stretching) appear, which confirm that cellulose is being oxidized during milling.

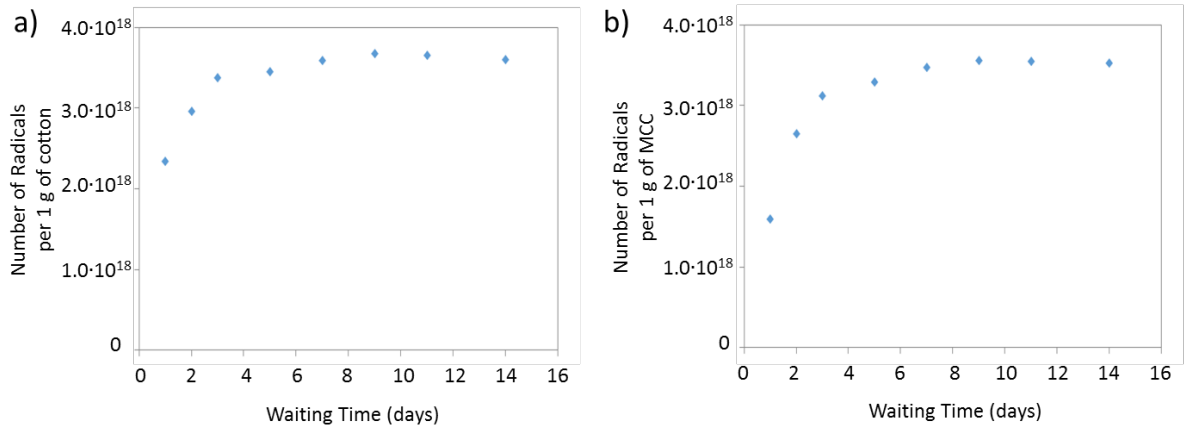

Figure S19. Number of radicals per gram of 'dry' milled 500 mg of a) cotton and b) MCC, calculated after the addition of DPPH solutions and waiting for the selected times. 0.5 g of cellulose sample (MCC or cotton) was cryomilled for 30 minutes at the frequency of 30 Hz. *Experimental procedure:* After grinding the cellulose samples, 2.5 mL of 1.3×10^{-3} M DPPH solution prepared in acetonitrile was added on the milled sample. Then the mixture was diluted to 10 mL by adding acetonitrile and stored in the dark. After indicated waiting time 0.5 mL of supernatant containing DPPH solution was diluted to 5 mL with acetonitrile and UV-Vis absorption spectra were recorded to assess, using Beer-Lambert law, the amount of DPPH reacted. This amount is equal to the amount of formed mechanoradicals.

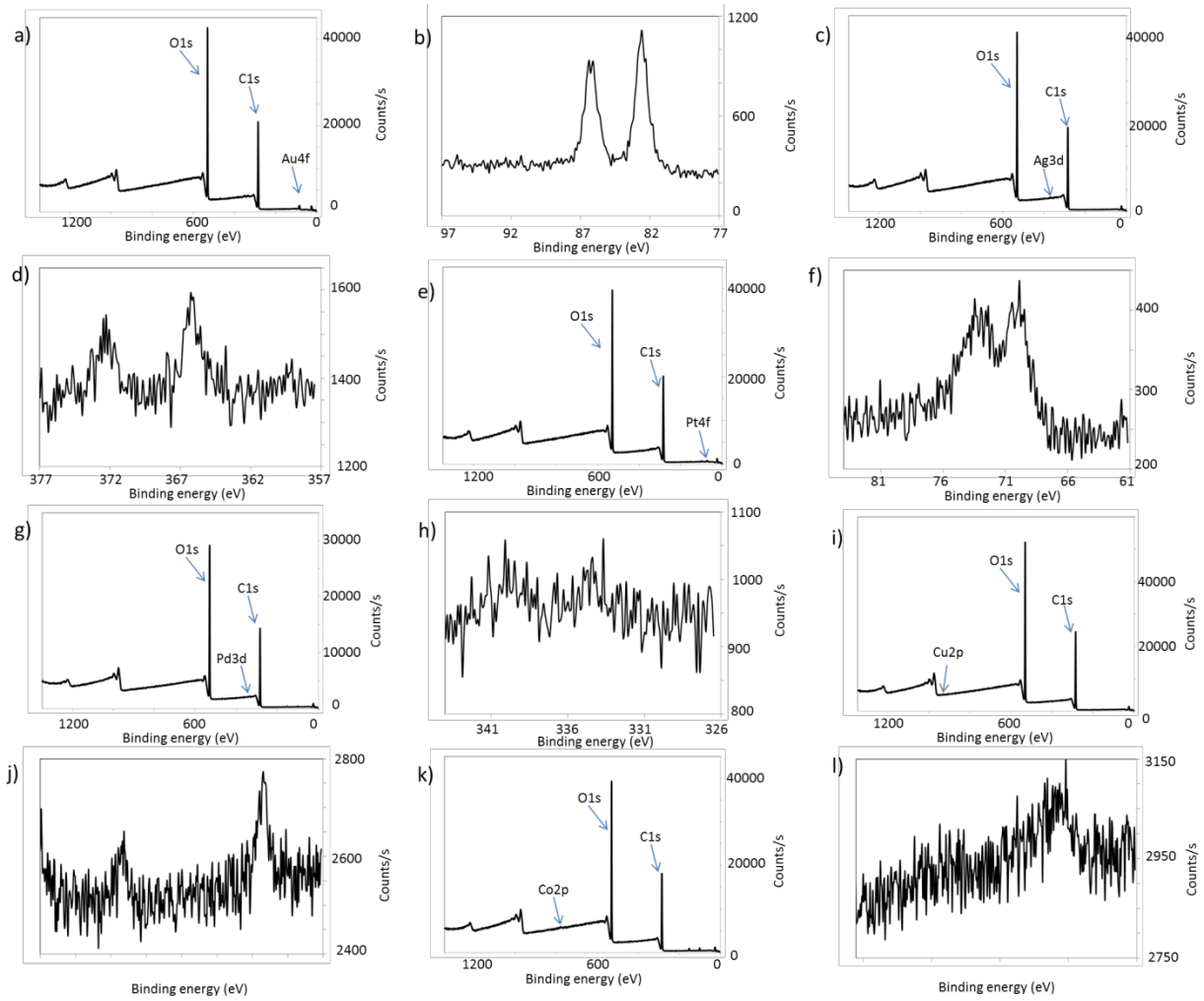

Figure S20. XPS survey a) cotton-Au, c) cotton-Ag, e) cotton-Pt, g) cotton-Pd, i) cotton-Cu, k) cotton-Co and HIRES XPS spectra of b) cotton-Au, d) cotton-Ag, f) cotton-Pt, h) cotton-Pd, j) cotton-Cu, l) cotton-Co nanocomposites (pellets) prepared by grinding 0.5 g of cotton at 30 Hz frequency in the presence of 6 zirconia balls in the zirconia sample chamber at 77 K for 30 minutes and then, adding metal ion solution (3 mL, 5.1×10^{-3} M, $HAuCl_4$, K_2PtCl_4, $AgNO_3$ in H_2O; $Pd(C_5H_7O_2)_2$ $Co(C_5H_7O_2)_2$, $Cu(C_5H_7O_2)_2$ in acetonitrile) (See Experimental section for more details). These spectra verify the metallic nature of the nanoparticles after pressing them into a pellet using a sample pellet press.

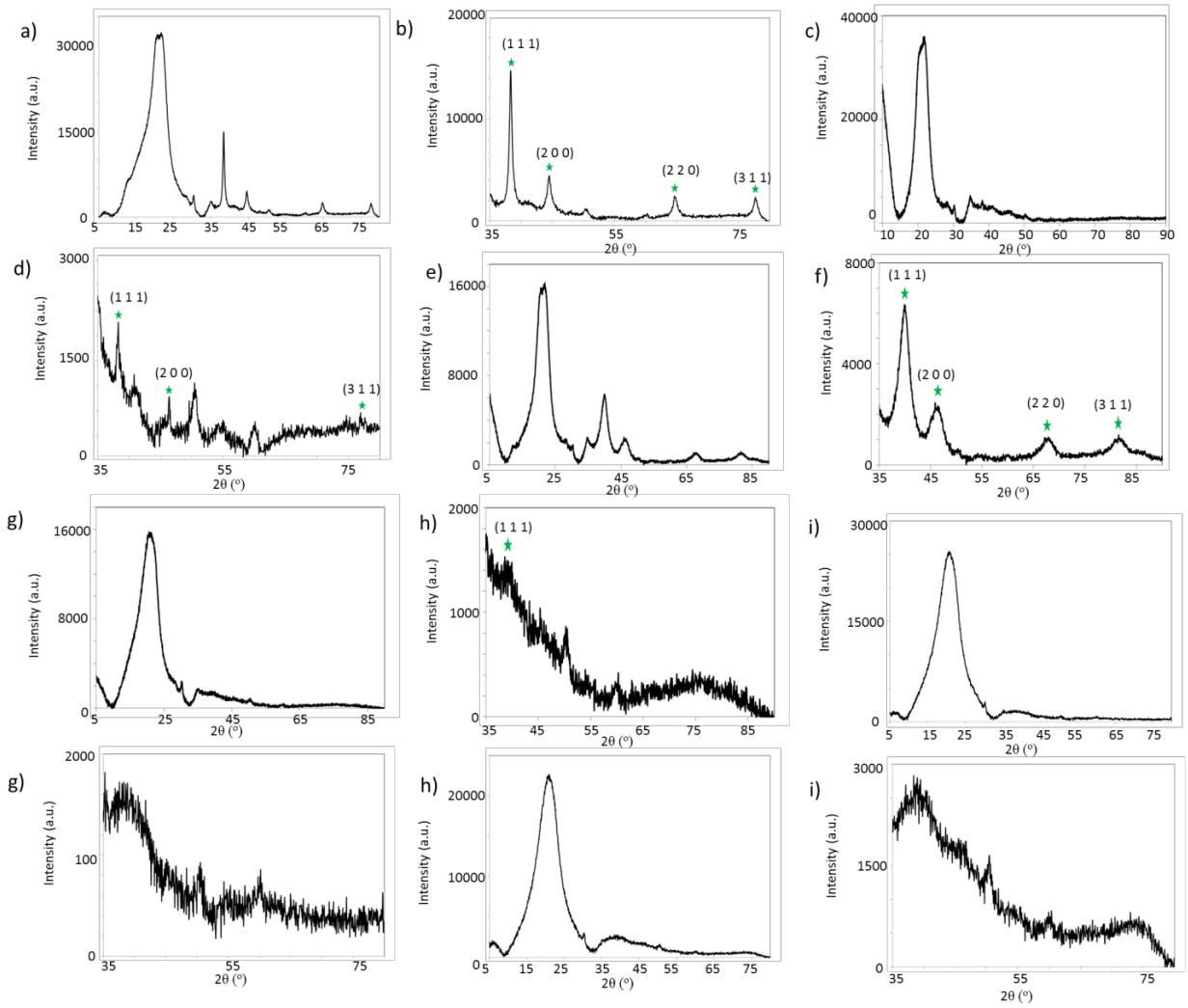

Figure S21. X-Ray diffractograms of a) and b) cotton-Au , c) and d) cotton-Ag, e) and f) cotton-Pt, g) and h) cotton-Pd, i) and j) cotton-Cu, k) and l) cotton-Co nanocomposites (pellets) prepared by grinding 0.5 g of cotton at 30 Hz frequency in the presence of 6 zirconia balls in the zirconia sample chamber at 77 K for 30 minutes and then, adding metal ion solution (3 mL, $5.1x10^{-3}$ M, $HAuCl_4$, K_2PtCl_4, $AgNO_3$ in H_2O; $Pd(C_5H_7O_2)_2$ $Co(C_5H_7O_2)_2$, $Cu(C_5H_7O_2)_2$ in acetonitrile) (See Experimental section for more details). These diffractograms verify the metallic nature of the nanoparticles (as evidenced by the appearance of the signals at the star labelled diffraction angles) after pressing them into a pellet using a sample pellet press.

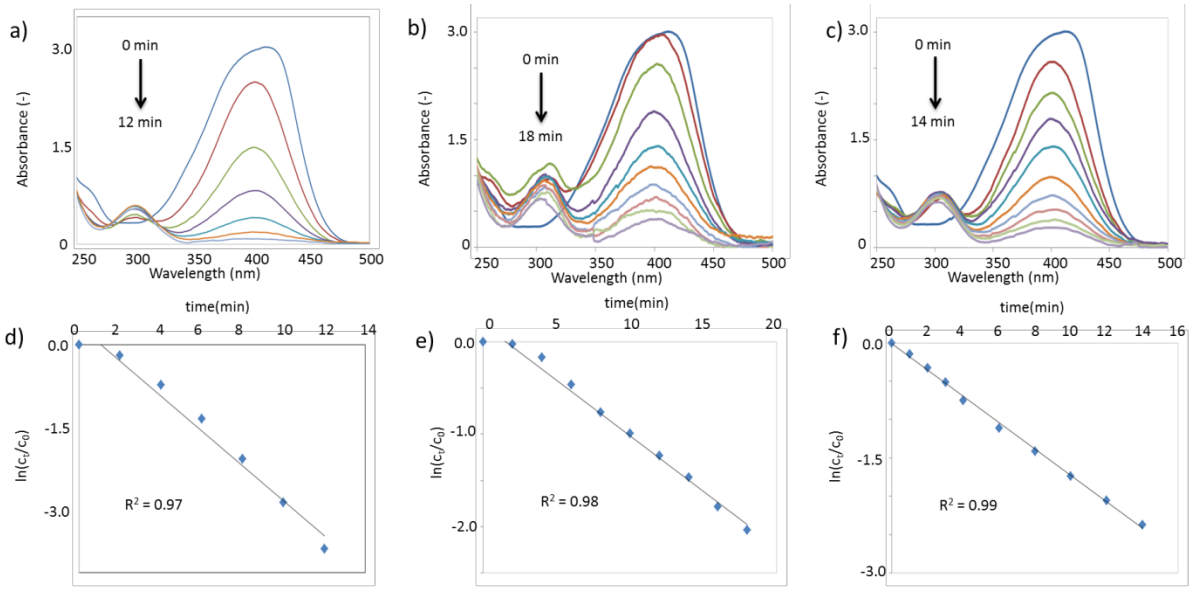

Figure S22. UV-Vis absorption spectra during the reduction of 4-NPh (0.3 mM in H_2O) to 4-APh in the presence of a) MCC-Ag NPs, b) MCC-Pt NPs, c) MCC-Pd NPs (1.0 mg composite in powder form); Graphs indicating the change of $\ln(C_t/C_0)$ with time during the reduction of 4-NPh in the presence of d) MCC-Ag NPs, e) MCC-Pt NPs, f) MCC-Pd NPs. (For more details on the reaction conditions, see Experimental Section).

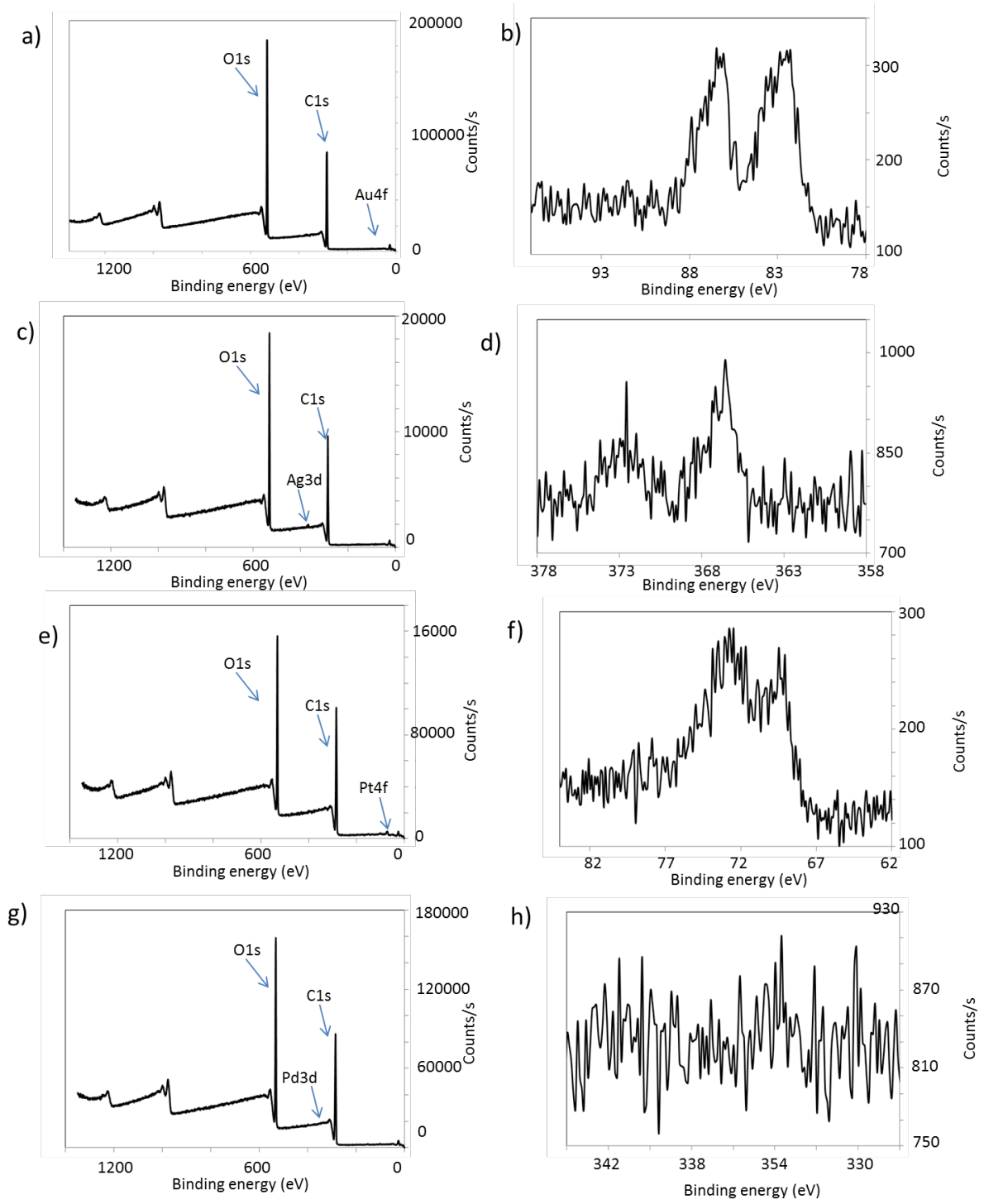

Figure S23. XPS survey of a) MCC-Au, c) MCC-Ag, e) MCC-Pt, g) MCC-Pd and HIRES XPS spectra of b) MCC-Au, d) MCC-Ag, f) MCC-Pt, h) MCC-Pd NPs after the reduction of 4-NPh to 4-APh in the presence of 1.0 mg of the composite. These spectra verify the metallic nature of the nanoparticles after using the composites as catalyst in the reduction of 4-NPh.

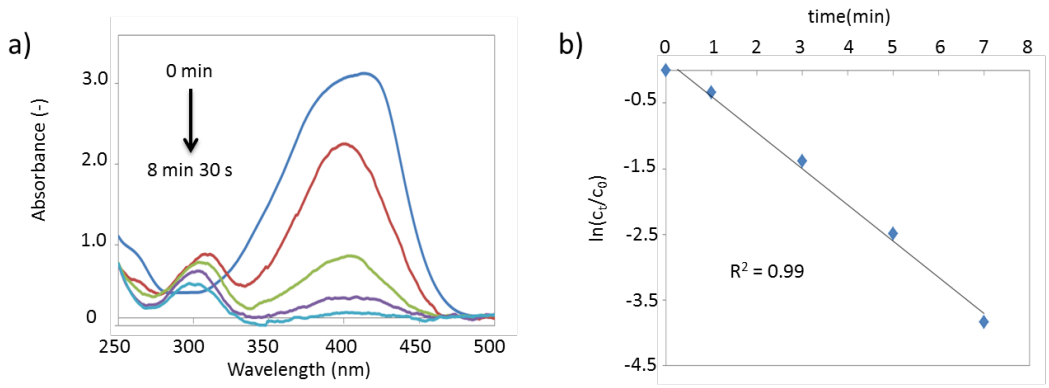

Figure S24. a) UV-Vis absorption spectra during the reduction of 4-NPh (0.3 mM in H_2O) to 4-APh in the presence of MCC-Au NPs (10.0 mg composite in powder form). b) Graph indicating the change of $\ln(C_t/C_0)$ with time during the reduction of 4-NPh in the presence of MCC-Au NPs.

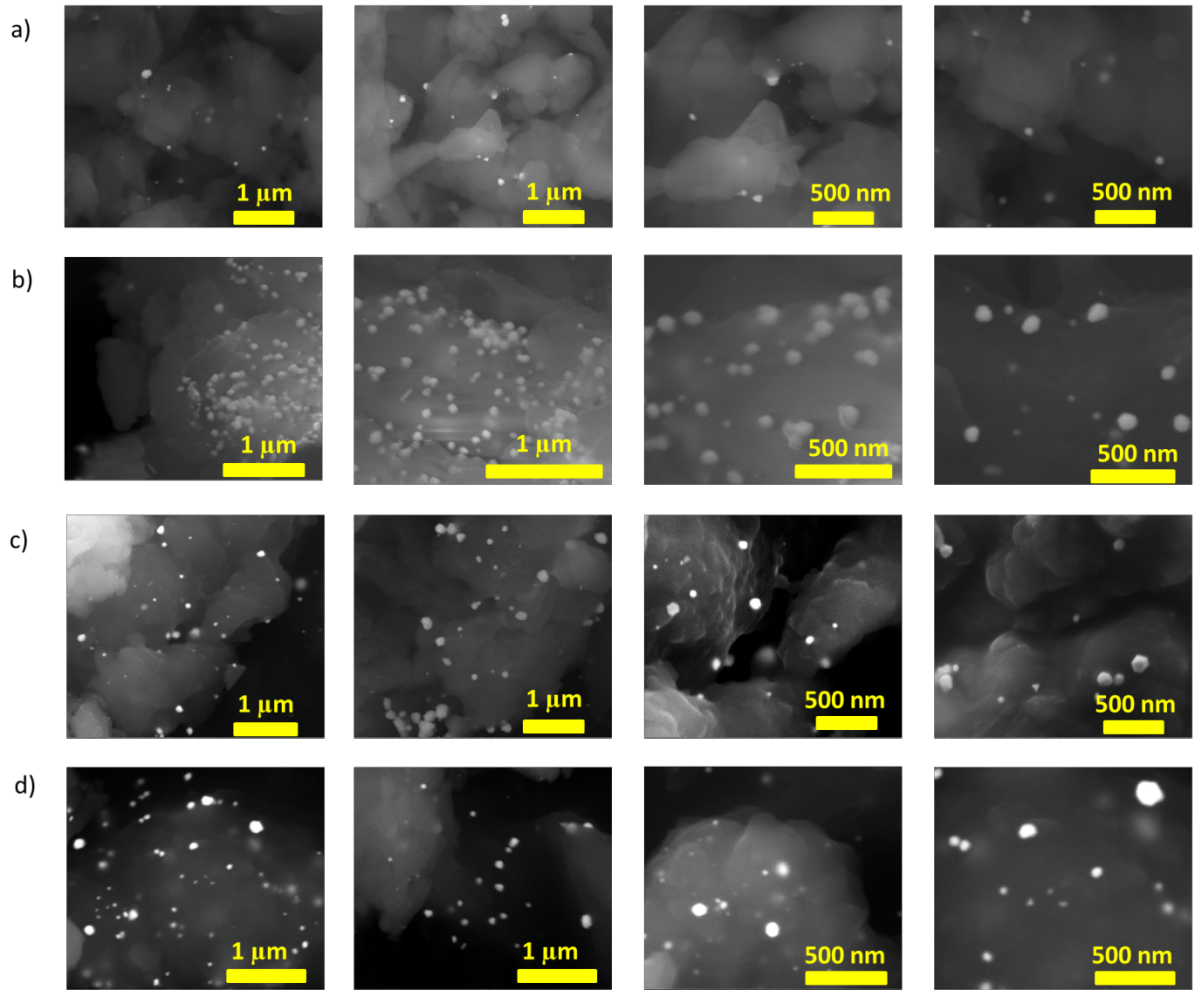

Figure S25. SEM images of a) cotton-PMMA-Au **1** (50% of PMMA, w/w), b) cotton-PMMA-Au **2** (25% of PMMA, w/w), c) cotton-PS-Au **1** (50% of PS, w/w), d) cotton-PS-Au **2** (25% of PS, w/w). These composites were prepared by grinding cotton and synthetic polymer for 30 minutes at 30 Hz frequency in the presence of 6 zirconia balls in the zirconia sample chamber at 77 K, after then adding $HAuCl_4$ solution in H_2O (3 mL, $5.1x10^{-3}$ M).

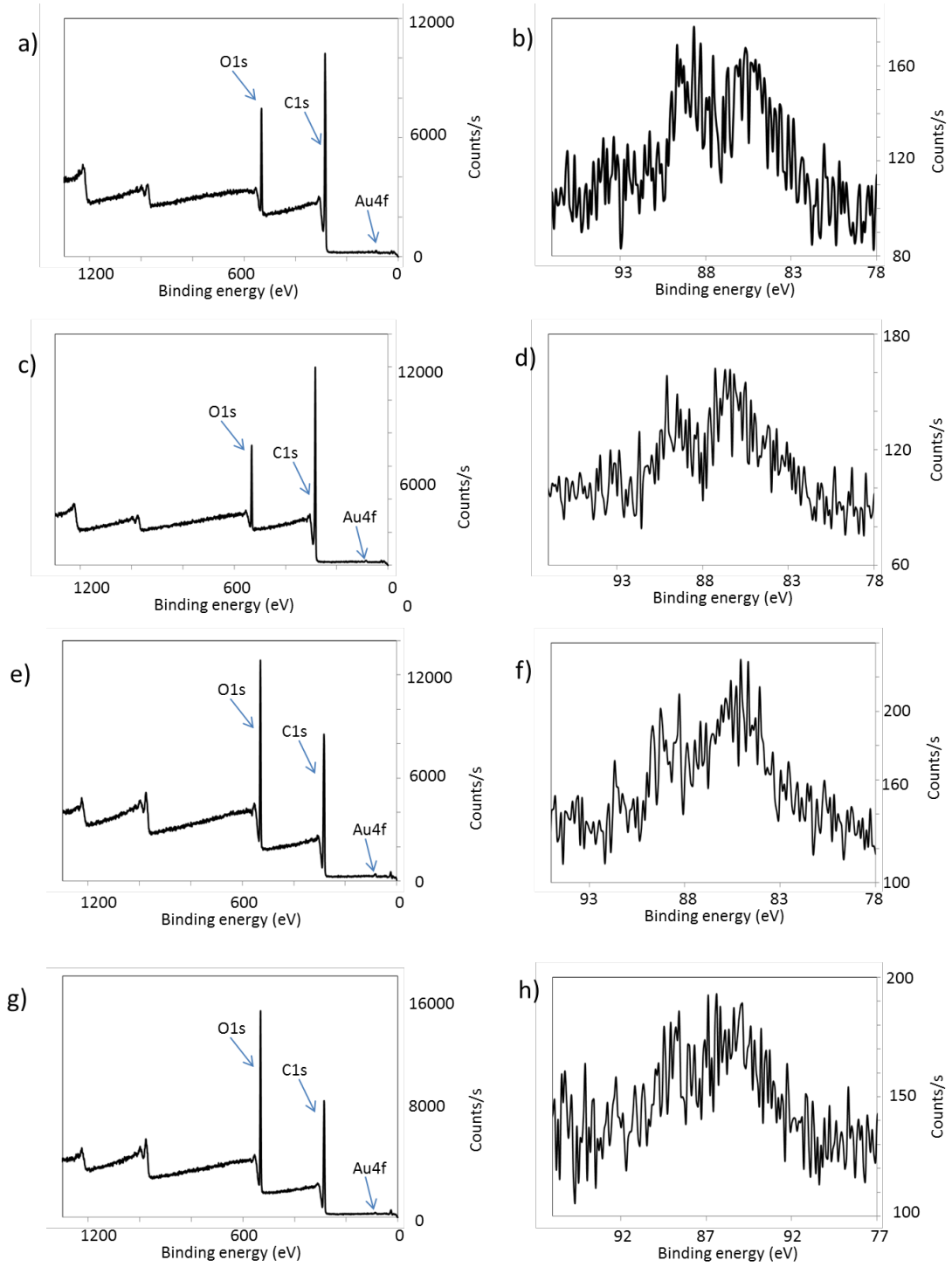

Figure S26. XPS survey a) cotton-PS-Au **2** (25% of PS, w/w), c) cotton-PS-Au **1** (50% of PS, w/w), e) cotton-PMMA-Au **2** (25% of PMMA, w/w), g) cotton-PMMA-Au **1** (50% of PMMA, w/w) and HIRES XPS spectra of b) cotton-PS-Au **2** (25% of PS, w/w), d) cotton-PS-Au **1** (50% of PS, w/w), f) cotton-PMMA-Au **2** (25% of PMMA, w/w), h) cotton-PMMA-Au **1** (50% of PMMA, w/w). These composites were prepared by grinding cotton and synthetic polymer for 30 minutes at 30 Hz frequency in the presence of 6 zirconia balls in the zirconia sample chamber at 77 K, after then adding $HAuCl_4$ solution in H_2O (3 mL, $5.1x10^{-3}$ M). The spectra verify the metallic nature of the nanoparticles – the successful reduction of the metal ion by the mechanoradicals.

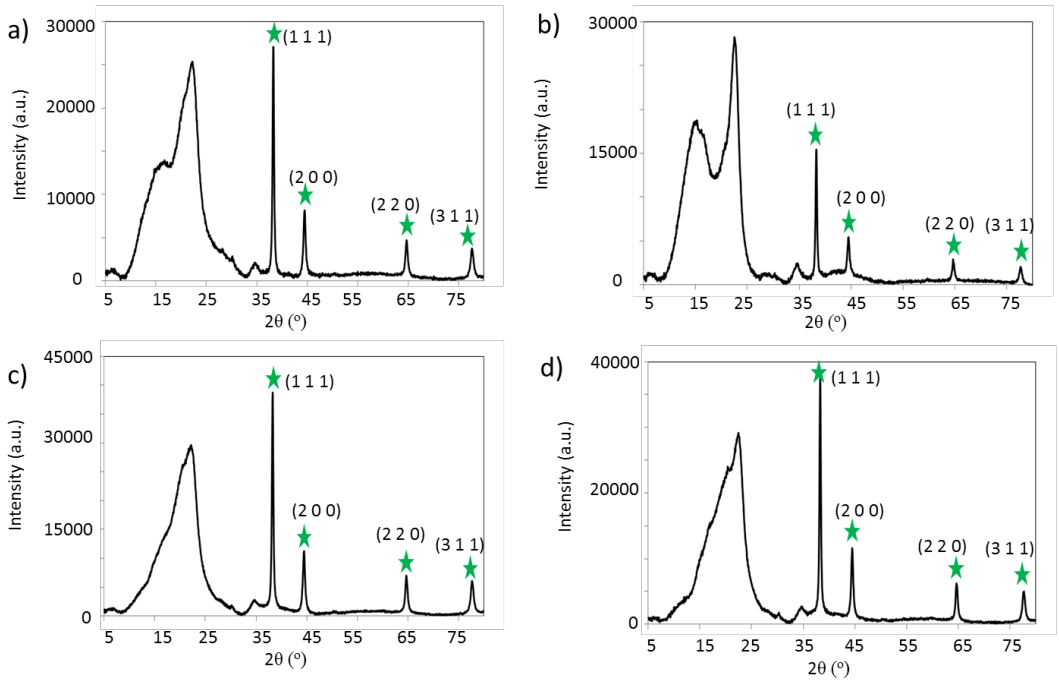

Figure S27. X-Ray diffratograms of a) cotton-PMMA-Au **2** (25% of PMMA, w/w), b) cotton-PMMA-Au **1** (50% of PMMA, w/w), c) cotton-PS-Au **2** (25% of PS, w/w), d) cotton-PS-Au **1** (50% of PS, w/w). These composites were prepared by grinding cotton and synthetic polymer for 30 minutes at 30 Hz frequency in the presence of 6 zirconia balls in the zirconia sample chamber at 77 K, after then adding $HAuCl_4$ solution in H_2O (3 mL, $5.1x10^{-3}$ M). The diffratograms verify the metallic nature of the nanoparticles, as evidenced by the appearance of the signals at the star labelled diffraction angles.

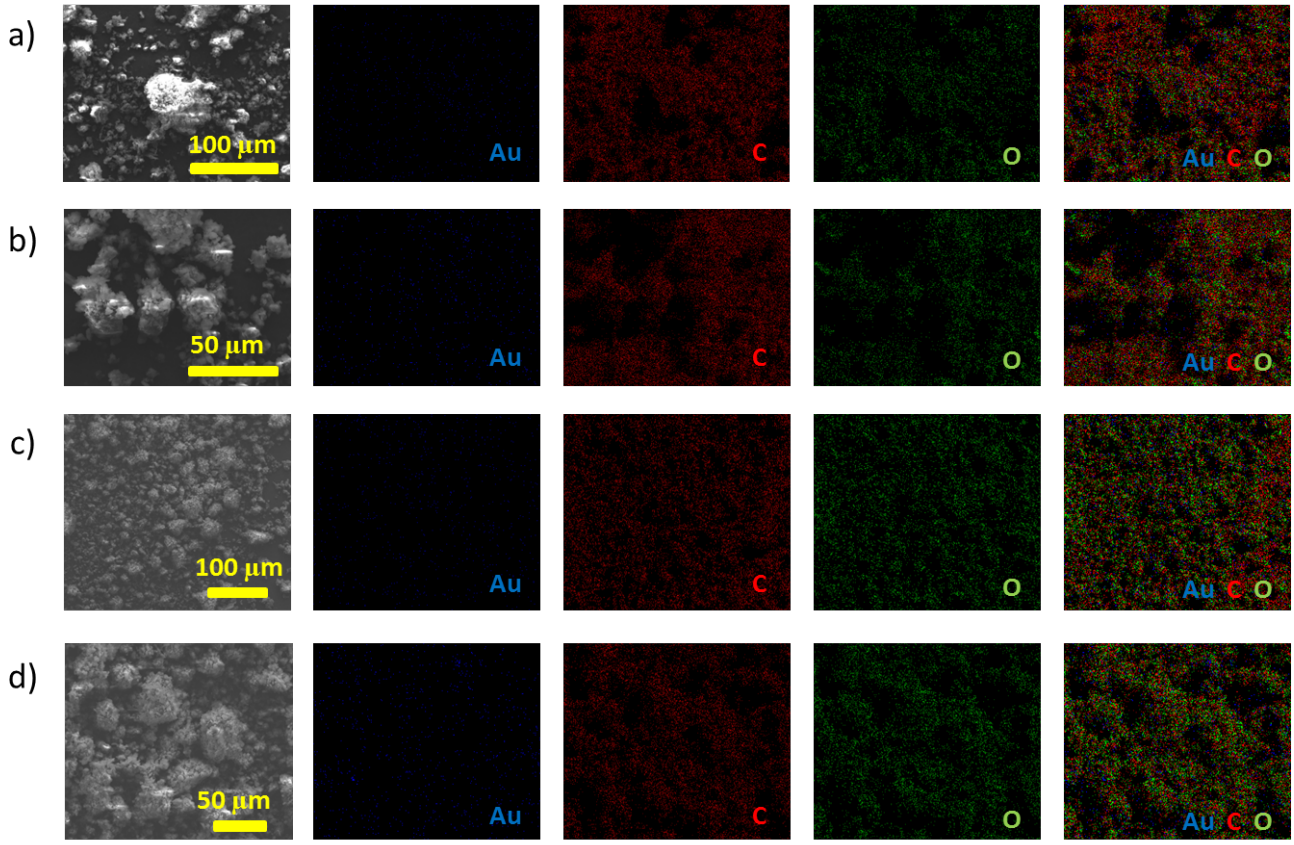

Figure S28. SEM-EDX elemental mapping of a) and b) cotton-PS-Au **1** (50% of PS, w/w), c) and d) cotton-PS-Au **2** (25% of PS, w/w). The maps confirmed the presence of C, O, and Au which indicated that cellulose and PS blended well with each other.

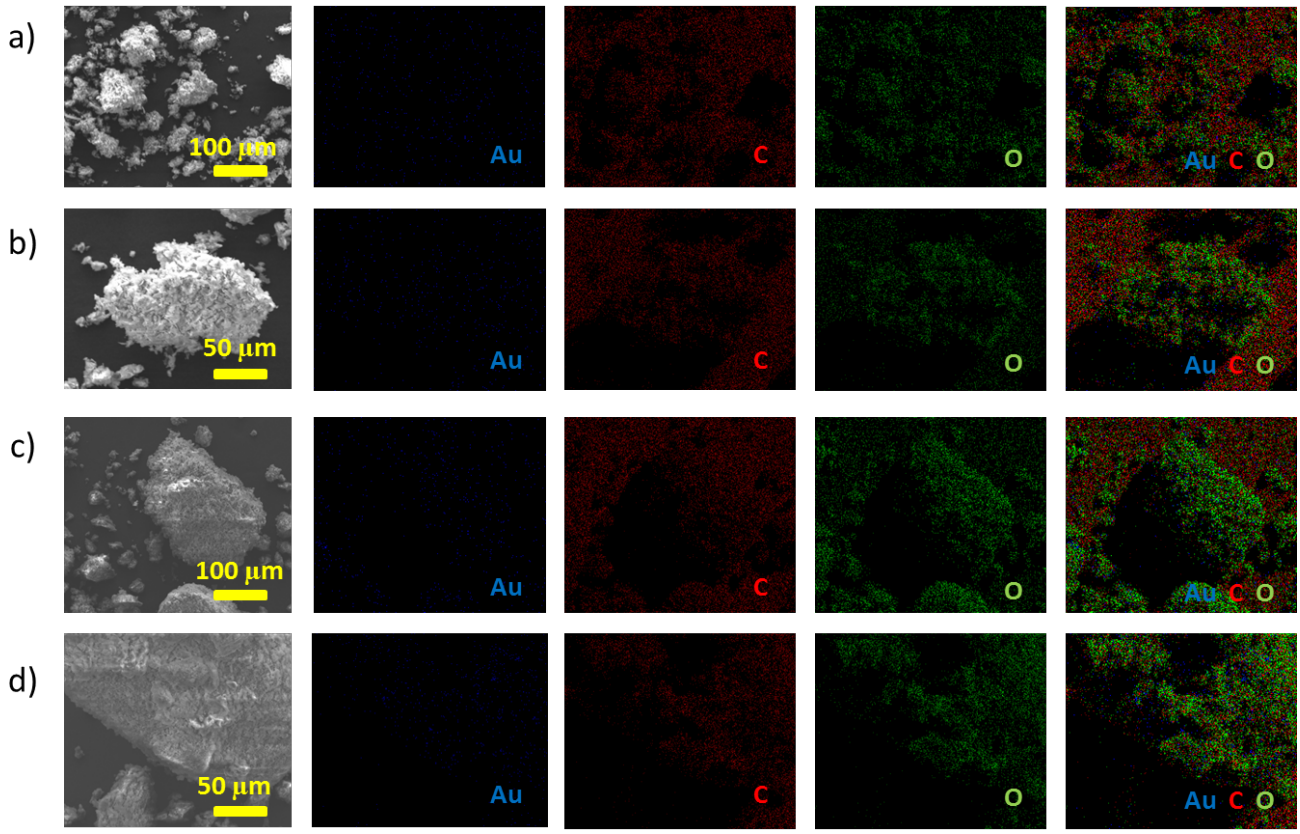

Figure S29. SEM-EDX elemental mapping of a) and b) cotton-PMMA-Au **1** (50% of PMMA, w/w), c) and d) cotton-PMMA-Au **2** (25% of PMMA, w/w). The maps confirmed the presence of C, O, and Au which indicated that cellulose and PMMA blended well with each other.

Table S1. Atomic percentage of metal in cotton-based nanocomposites as determined by XPS (See Supplementary text for more details).

Nanocomposite	at. % (after indicated time of storage in metal salt solutions)		
	1 day	1 week	2 weeks
cotton-Au NPs	0.148 ± 0.008	0.176 ± 0.002	0.184 ± 0.025
cotton-Ag NPs	0.013 ± 0.001	0.132 ± 0.018	0.167 ± 0.015
cotton-Pd NPs	0.021± 0.005	0.028 ± 0.003	0.034 ± 0.008
cotton-Pt NPs	0.051 ± 0.001	0.081 ± 0.008	0.142 ± 0.058

Table S2. Concentration of metals as obtained from ICP-MS measurements, and metal content in 500 mg of composite.

Nanocomposite	Metal concentration [mg/L]	Metal content in 500 mg of composite [mg]
MCC-Au NPs	18.8 ± 0.3	1.88
MCC-Ag NPs	2.6 ± 0.1	0.20
MCC-Pd NPs	0.61 ± 0.02	0.06
MCC-Pt NPs	16.1 ± 0.1	1.61
MCC-Au NPs (after 1st catalytic cycle)	18.0 ± 0.5	1.80
MCC-Au NPs (after 2nd catalytic cycle)	17.3 ± 0.1	1.73
Cotton-Au NPs	24.6 ± 0.7	2.46
Cotton-Ag NPs	1.86 ± 0.02	0.14
Cotton-Pd NPs	0.57 ± 0.02	0.06
Cotton-Pt NPs	15.7 ± 0.3	1.57

Table S3. Surface resistivity and conductivity of nanocomposites.

material	R_s (Ω)	ρ_s (S)	Ratio of ρ_s of nanocomposite and ρ_s of cotton
cotton	$9.88 \cdot 10^{13} \pm 7.12 \cdot 10^{12}$	$1.02 \cdot 10^{-13} \pm 7.52 \cdot 10^{-16}$	-
cotton-Au NPs	$1.82 \cdot 10^{12} \pm 7.12 \cdot 10^{11}$	$6.15 \cdot 10^{-13} \pm 2.10 \cdot 10^{-13}$	38.1
cotton-Ag NPs	$3.38 \cdot 10^{12} \pm 7.12 \cdot 10^{11}$	$3.08 \cdot 10^{-13} \pm 7.02 \cdot 10^{-14}$	19.0
cotton-Pt NPs	$8.58 \cdot 10^{12} \pm 1.74 \cdot 10^{12}$	$1.21 \cdot 10^{-13} \pm 2.46 \cdot 10^{-14}$	7.5
cotton-Pd NPs	$4.16 \cdot 10^{12} \pm 5.81 \cdot 10^{11}$	$2.44 \cdot 10^{-13} \pm 2.87 \cdot 10^{-14}$	15.1
cotton-Co NPs	$9.10 \cdot 10^{12} \pm 1.84 \cdot 10^{12}$	$1.13 \cdot 10^{-13} \pm 2.08 \cdot 10^{-14}$	7.0
cotton-Cu NPs	$5.46 \cdot 10^{12} \pm 5.81 \cdot 10^{11}$	$1.85 \cdot 10^{-13} \pm 1.72 \cdot 10^{-14}$	11.4

Table S4. Concentration of Ag^+ released from cotton and MCC supported nanocomposites obtained from ICP-MS measurements (See Figure 3 of the main text and Experimental Section for further details).

Nanocomposite	concentration of Ag^+ ($\mu g \cdot L^{-1}$)
cotton-Ag NPs	669.20 ± 2.01
MCC-Ag NPs	180.82 ± 2.96

References:

1 R. Robert, S. Barbati, N. Ricq and M. Ambrosio, *Water Research*, 2002, **36**, 4821–4829.
2 K. L. McGilvray, M. R. Decan, D. Wang and J. C. Scaiano, *J. Am. Chem. Soc.*, 2006, **128**, 15980–15981.
3 J. Belloni, M. Mostafavi, H. Remita, J.-L. Marignier and and M.-O. Delcourt, *New J. Chem.*, 1998, **22**, 1239–1255.
4 G. K. Inwati, Y. Rao and M. Singh, *Nanoscale Res Lett*, 2016, **11**, 458.